Third-order nonlinear optical susceptibility and photoluminescence in porous silicon

Yoshihiko Kanemitsu and Shinji Okamoto
Institute of Physics, University of Tsukuba, Tsukuba, Ibaraki 305, Japan

Akihiro Mito
National Research Laboratory of Metrology, Tsukuba, Ibaraki 305, Japan
(Received 22 May 1995)

Third-order nonlinear-optical-susceptibility spectra $|\chi^{(3)}(-3\omega;\omega,\omega,\omega)|$ have been obtained for free-standing porous silicon films by third-harmonic-generation (THG) measurements in a third-harmonic photon energy region from 540 to 720 nm, which covers the visible photoluminescence (PL) wavelength region. In the THG wavelength region between 540 and 720 nm, the $|\chi^{(3)}|$ spectrum is not sensitive to the excitation laser wavelength and shows about 0.5×10^{-12} esu. This suggests that there is no excitonic resonance enhancement of the $|\chi^{(3)}|$ spectrum in the PL wavelength region. The optical absorption and luminescence properties of porous silicon are discussed.

Since the discovery of efficient visible photoluminescence (PL) from Si,[1] Ge,[2] and SiC nanocrystallines,[3] there have been numerous reports describing visible luminescence properties of nanocrystallites made from indirect-gap IV and IV-IV semiconductors. In particular, porous silicon[4] is receiving widespread interest motivated by potential applications as light-emitting devices. However, despite the large number of theoretical and experimental reports on visible luminescence in porous silicon, there is no consensus for the mechanism of efficient visible luminescence at room temperature.[5] The blueshift of the absorption spectra in porous silicon[6] shows that the quantum-confinement effect affects the electronic structure of nanocrystallites. On the other hand, a drastic size reduction to a few nanometers is needed for the observation of efficient visible luminescence. Since a large fraction of silicon atoms appears on the surface, the surface states on the Si nanocrystallites also play an active role. In fact, the luminescence properties of porous silicon are sensitive to the surface chemistry of nanocrystallites.[5] The mechanism of visible luminescence is under discussion: band-edge emission (light emission from the crystalline core state; the pure quantum-confinement model) (Refs. 7 and 8) or localized state emission (light emission from surface localized states; the quantum-confinement model with surface state effects).[9–11]

Porous silicon shows complicated optical behaviors. Porous silicon is inhomogeneous in the sense that it has a distribution of the crystallite size and shape, and variations in surface structures and surface stoichiometry. In inhomogeneous systems, nonlinear optical measurements provide detailed information on electronic structures. The infrared up-conversion experiment implies that, under 1.06-μm excitation, third-harmonic radiation (355 nm) is efficiently generated, and acts as a pump source to excite visible photoluminescence in porous silicon.[12] Pump-and-probe experiments[13,14] show that the nonlinear absorption coefficient depends on the pump laser wavelength, and that the photogeneration of carriers occurs efficiently at laser wavelengths shorter than 500 nm. The study of nonlinear optical properties will open an approach to discuss the origin and mechanism of efficient visible luminescence in porous silicon.

In this work, we measured third-order nonlinear-optical-susceptibility $|\chi^{(3)}|$ spectra in porous silicon films by third-harmonic generation (THG) Maker fringe method for a third-harmonic photon energy region from 540 to 720 nm, which covers the visible luminescence region. No significant structure in the $|\chi^{(3)}|$ spectrum is observed in the photoluminescence wavelength region. It is considered that porous silicon has an indirect-gap semiconductor nature in the optical-absorption process, and that the red luminescence comes from surface-localized states rather than the delocalized crystalline core.

The porous silicon layers were formed by electrochemical anodization. The substrates were (100)-oriented 3.5–4.5-Ω cm resistivity p-type silicon. Thin Al films were evaporated on the back of the wafers to form a good Ohmic contact. The anodization was carried out in HF-ethanol solution ($HF:H_2O:C_2H_5OH = 1:1:2$) at constant current density in the range of 10 mA/cm^2 for 10 min. After anodization, the sample was rinsed in deionized water for several minutes. Then the sample was oxidized by exposing it to air to obtain stable photoluminescence with higher quantum efficiency.[7] Raman spectroscopy and transmission electron microscopy indicate that the average diameter of nanometer-sized Si crystallites was about 3 nm.[6] The porous silicon films were sandwiched by two SiO_2 glasses.

The ordinary one-photon absorption spectrum in a porous silicon film is shown in Fig. 1. In our samples, there is no significant absorption from 600 nm to 3 μm. The inset of the figure shows the photoluminescence spectrum under 325-nm excitation. Broad photoluminescence was observed in the red spectral region around 700 nm. In order to discuss the mechanism of efficient red luminescence, we need to determine the band edge in porous silicon. However, it is hard to determine the band-gap energy or the absorption onset from the absorption measurement exactly, because featureless absorption

0163-1829/95/52(15)/10752(4)/$06.00

spectra depending the crystallite size are observed.[6] These featureless absorption spectra in indirect-gap semiconductor crystallites are intrinsic rather than inhomogeneity.[15] Therefore, using nonlinear-optical techniques, we tried to clarify whether the effective band of porous silicon exists in the broad PL spectrum (PL at room temperature is the band-edge emission) or not.

The THG Maker fringe method[16] was employed to evaluate the value of $|\chi^{(3)}(-3\omega;\omega,\omega,\omega)|$ as a function of fundamental photon energy. A difference frequency was generated between 1.6 and 2.1 μm by mixing a Q-switched Nd:YAG (yttrium aluminum garnet) laser and a dye laser using a $LiNbO_3$ crystal and was used as a pump light of the THG measurements. The pulse width was about 5 ns, and the repetition rate was 10 Hz. The near-infrared beam was split into two beams: pump light for sample excitation and reference light. The THG signals were detected by photomultipliers through pass filters, and then integrated by a boxcar averager. The sample signal was normalized pulse by pulse by the reference signal. Samples were kept in the center of a vacuum chamber with 500-mm length. The THG signal was calibrated by replacing the sample with SiO_2 glass at each wavelength. Moreover, we tried to determine the refractive index using an ellipsometer.

Figure 2 shows a typical example of the Maker fringe pattern; that is, the THG intensities as a function of the incident angle of the fundamental laser beam for a 42-μm-thick porous silicon. At large angles, a fringe pattern

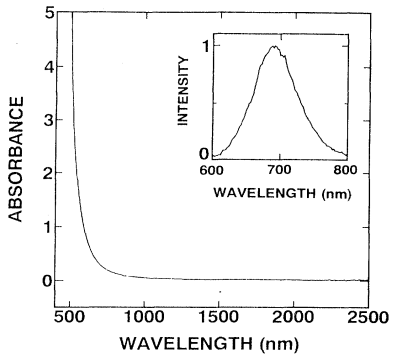

FIG. 1. Optical-absorption spectrum in a free-standing porous silicon film. The inset shows the photoluminescence under 325-nm laser excitation.

is clearly observed. To our knowledge, this is the first observation of the THG Maker fringe pattern in porous silicon. Even in a nanoscopic complex system such as porous silicon, the THG Maker fringe method is a useful one for the study of nonlinear optical properties.

Optical harmonic generation from a multilayered sample was treated by Bethune[17] using a transfer-matrix technique. Using this technique, we tried to calculate the THG Maker fringe pattern from a multilayered sample structure composed of a porous silicon film and two SiO_2 glasses. The THG amplitude is given by

$$E_7^+ \propto \left[\frac{\chi_4^{(3)}}{N_{4s(3)}^2-N_4^2}\right]\left[\frac{(\phi_4^{-1}\phi_{4s(3)}-1)t_{45}t_{56}t_{67}(E_{4s}^+)^3}{t_{4s(3)}(1+\phi_4^2 r_{34}r_{45})}\right] + \left[\frac{3\chi_4^{(3)}}{N_{4s(1)}^2-N_4^2}\right]\left[\frac{(\phi_4^{-1}\phi_{4s(1)}-1)t_{45}t_{56}t_{67}(E_{4s}^+)^2E_{4s(1)}^-}{t_{4s(1)}(1+\phi_4^2 r_{34}r_{45})}\right],$$

where the suffix 1 denotes the vacuum (fundamental laser input side), 2 the SiO_2 glass, 3 the vacuum, 4 the porous silicon sample, 5 the vacuum, 6 the SiO_2 glass, and 7 the vacuum (laser output side); the suffix + denotes the forward propagation wave and − the backward; the subscript s indicates a quantity associated with the nonlinear polarization which provides the source current of THG; the superscript ′ indicates the parameters for the fundamental wavelength; and the others are for the THG wavelength. $r_{ij}[=(N_i-N_j)/(N_i+N_j)]$ and $t_{ij}[=2N_j(N_i+N_j)]$ are the reflection and transmission amplitudes for light upon the $i-j$ interface from medium i. The parameters N_j and N_j' are given by

$$N_j=[n_j(3\omega)^2-\sin^2(\theta)]^{1/2}$$

and

$$N_j'=[n_j(\omega)^2-\sin^2(\theta)]^{1/2},$$

where θ is the angle of incidence and $n_j(=n+ik)$ is the complex refractive index; $\phi_j=\exp(iN_jk_0d_j)$ and $\phi_j'=\exp(iN_j'k_0d_j)$, where $k_0=\omega/c$ and d_j is the layer thickness; $N_{js(3)}=N_j'$ and $N_{js(1)}=N_j'/3$. The forward and backward fundamental beam amplitudes E_{4s}^+ and E_{4s}^- from a porous silicon film are

$$E_{4s}^+=\frac{t_{12}'t_{23}'t_{34}'}{1+\phi_4'^2 r_{34}'r_{45}'}$$

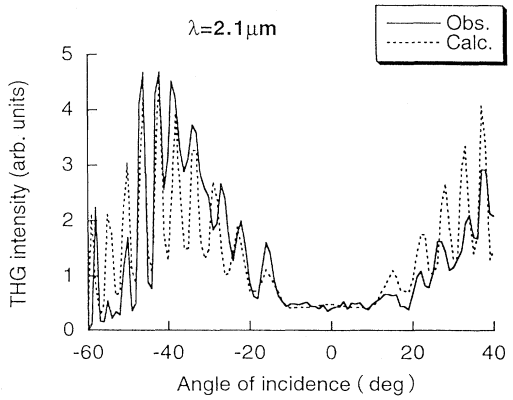

FIG. 2. Typical third-harmonic intensity pattern for a porous silicon film as a function of incident angle of the fundamental pulse laser light to the sample (solid line). The broken line is the theoretically calculated fringe pattern.

and

$$E_{4s}^{-}=\frac{t'_{12}t'_{23}t'_{34}r'_{45}\phi'^{2}_{4}}{1+\phi'^{2}_{4}r'_{34}r'_{45}} .$$

The THG signal is proportional to $|E_7^+|^2$. Using the above equations, we calculated the Maker fringe patterns, and an example is shown in Fig. 2. Here the THG amplitudes from the SiO_2 glasses are neglected because this effect is small. The periods of the fringe patterns in the experiment are reproduced by the theoretical calculations, and we can evaluate the value of $|\chi^{(3)}|$ at a given wavelength.

The third-order nonlinear-optical-susceptibility $|\chi^{(3)}|$ spectrum as a function of the THG wavelength is summarized in Fig. 3. The value of $|\chi^{(3)}|$ is not sensitive to the pump laser wavelength. The value of $|\chi^{(3)}|$ is about 0.5×10^{-12} esu in this region, where the $|\chi^{(3)}|=1.0\times10^{-14}$ esu of fused silica is adopted as a standard value.[16] The $\chi^{(3)}$ value is not determined uniquely at a given wavelength, because a few parameters $\chi^{(3)}$, $n(\omega)$, and $\Delta n(\omega)=n(3\omega)-n(\omega)$ give the same minima of the least-squares fit. Typical values of $n(\omega)\sim1.5$ and $\Delta n\sim0.05$ are determined at each wavelength. We note that $\chi^{(3)}/\Delta n(\omega)$ value is more constant in determination. The scattering of data is caused mainly by the fitting procedure between the experimental and theoretical fringe patterns. We find that porous silicon has a large value of $\chi^{(3)}$, although the absorption coefficient is very small and the refraction index ($n\sim1.5$) is low in the near-infrared wavelength region.

In direct-gap semiconductor nanocrystallites such as CuCl or CuBr quantum dots, the $|\chi^{(3)}|$ spectrum exhibits sharp peaks at exciton states near the absorption edge: Resonance enhancement of $|\chi^{(3)}|$ due to exciton confinement is clearly observed in the luminescence wavelength region (near the band edge).[18] In porous silicon, no sign of enhancement effect in $|\chi^{(3)}|$ is observed in the luminescence spectral region. This fact provides important information on optical-absorption and luminescence processes in porous silicon. Two possibilities can be pointed out. First, the indirect-gap nature is important in the optical transition. Porous silicon has an indirect-gap semiconductor nature, and the lowest optical transition is the phonon-assisted optical transition near the absorption edge.[7,8,19] Then it is speculated that the enhancement of $|\chi^{(3)}|$ is not observed near the indirect-transition region. Second, we can consider that there is no resonant enhancement due to the band edge in this wavelength region, and the band gap is above this THG photon energy region. The red photoluminescence with a peak of ~700 nm is the light emission from localized states with small density of states, rather than the band-edge emission.

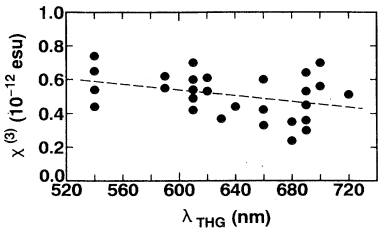

FIG. 3. Third-order nonlinear-optical-susceptibility $|\chi^{(3)}|$ spectrum as a function of the wavelength of the third-harmonic generation.

Porous silicon shows strong visible luminescence under wavelengths shorter than ~500 nm. The short THG light ($\lambda_{THG}<500$ nm) acts as a pump source to excite visible photoluminescence in porous silicon.[12] Furthermore, pump-and-probe experiments[14] show that large photoinduced absorption signals related to the photocarrier generation (the imaginary part of $\chi^{(3)}$) are observed, but that these signals are also insensitive to pump wavelengths longer than 550 nm. This result is consistent with the above-THG Maker fringe result. However, the induced absorption change at probe wavelengths of 600–800 nm is clearly observed when the excitation wavelength is shorter than 600 nm.[20] These results are explained by a picture in which photocarriers generated at the excitation laser wavelength are localized at lower-energy states, and then localized carriers cause a large absorption change in the luminescence wavelength region. Nonlinear-optical measurements imply that an effective band edge exists above the luminescence peak energy.[21] Therefore, from third-order nonlinear-optical-susceptibility measurements, it is considered that porous silicon has an indirect-gap semiconductor nature in the optical-absorption process, and that efficient room-temperature PL comes from lower-energy localized states with small density of states, rather than the band-edge emission.

In conclusion, we measured third-order nonlinear-optical-susceptibility spectra in porous silicon films by the third-harmonic generation (THG) Maker fringe method for a third-harmonic photon energy region, which covers the visible luminescence region. Porous silicon has unique nonlinear optical properties such as a relatively large $\chi^{(3)}$ in a transparent wavelength region. The study of nonlinear optical properties open an approach to discover unique optical properties other than visible luminescence, and to understand the electronic states and luminescence mechanism in porous silicon.

This work was partly supported by the Inamori Foundation and the Scientific Research Grant-In-Aid from Ministry of Education, Science and Culture, Japan.

[1]H. Takagi, H. Ogawa, Y. Yamazaki, A. Ishizaki, and T. Nakagiri, Appl. Phys. Lett. **56**, 2379 (1990).

[2]Y. Maeda, N. Tsukamoto, Y. Yazawa, and Y. Kanemitsu, Appl. Phys. Lett. **59**, 3168 (1991).

[3]T. Matsumoto, J. Takahashi, T. Tamaki, T. Futagi, H. Mimura, and Y. Kanemitsu, Appl. Phys. Lett. **64**, 226 (1994).

[4]L. T. Canham, Appl. Phys. Lett. **57**, 1046 (1990).

[5]See, for example, D. J. Lockwood, Solid State Commun. **92**,

101 (1994).
[6]Y. Kanemitsu, H. Uto, Y. Masumoto, T. Matsumoto, T. Futagi, and H. Mimura, Phys. Rev. B **48**, 2827 (1993).
[7]P. D. J. Calcott, K. J. Nash, L. T. Canham, M. J. Kane, and D. Brumhead, J. Phys. Condens. Matter **5**, L91 (1993).
[8]T. Suemoto, K. Tanaka, and A. Nakajima, in *Light Emission from Novel Silicon Materials,* edited by Y. Kanemitsu, M. Kondo, and K. Takeda (The Physical Society of Japan, Tokyo, 1994), p. 190.
[9]Y. Kanemitsu, T. Ogawa, K. Shiraishi, and K. Takeda, Phys. Rev. B **48**, 4883 (1993).
[10]S. M. Prokes, W. E. Carlos, and O. J. Glembocki, Phys. Rev. B **50**, 17 093 (1994).
[11]F. Koch and V. Petrova-Koch, in *Porous Silicon,* edited by Z. C. Feng and R. Tsu (World Scientific, Singapore, 1994), p. 133.
[12]J. Wang, H. B. Jiang, W. C. Wang, J. B. Zheng, F. L. Zang, P. H. Hao, X. Y. Hou, and X. Wang, Phys. Rev. Lett. **69**, 3252 (1993).
[13]T. Matsumoto, N. Hasegawa, T. Tamaki, K. Ueda, T. Futagi, H. Mimura, and Y. Kanemitsu, Jpn. J. Appl. Phys. **33**, L35 (1994).
[14]T. Matsumoto, T. Futagi, N. Haegawa, H. Mimura, and Y. Kanemitsu, in *Semiconductor Silicon 1994,* edited by H. R. Huff, W. Berghotz, and K. Sumino (Electrochemical Society, Pennington, NJ, 1994), p. 545.
[15]S. H. Tolbert, A. B. Herhold, C. S. Johnson, and A. P. Alivisatos, Phys. Rev. Lett. **73**, 3266 (1994).
[16]A. Mito, C. Takahashi, H. Matsuda, S. Okada, and H. Nakanishi, in *Proceedings of the International Conference on Lasers '92,* edited by C. P. Wang (STS, McLean, VA, 1993), p. 908.
[17]D. S. Bethune, J. Opt. Soc. Am. B **6**, 910 (1989).
[18]A. Namamura, Y. L. Lee, T. Kataoka, and T. Tokizaki, J. Lumin. **60/61**, 376 (1994).
[19]M. S. Hybertsen, Phys. Rev. Lett. **72**, 1514 (1994).
[20]T. Matsumoto (private communication); P. M. Fauchet, in *Microcrystalline and Nanocrystalline Semiconductors,* edited by L. Brus, M. Hirose, R. W. Collins, F. Koch, and C. C. Tsai, MRS Symposia Proceedings No. 358 (Materials Research Society, Pittsburgh, 1995), p. 525; (private communication).
[21]Here the effective band gap means the band gap of the set of nanocrystsallites in the porous silicon sample. Since porous silicon has a distribution and variations in surface structures and is a nanoscopic disordered system, the effective band gap reflects the size dispersion and surface structures of nanocrystallite.